Desalination and Water Treatment
www.deswater.com

doi: 10.1080/19443994.2015.1108240

57 (2016) 20511–20519
September

Taylor & Francis
Taylor & Francis Group

Removal of o-Cresol from aqueous solution using Algerian Na-Clay as adsorbent

Hayat Herbache[a], Amina Ramdani[a], Asmaa Maghni[a], Zoubida Taleb[a], Safia Taleb[a,*], Emilia Morallon[b], Rachid Brahmi[c]

[a]*Laboratory of Materials & Catalysis, Faculty of Sciences, Djillali Liabès University, Site I, B.P. 89, Sidi Bel-Abbès 22000, Algeria, Tel. +213 771218808; Fax: +213 48540360; email: safiatal@yahoo.fr (S. Taleb)*
[b]*Departamento de Química Física, Instituto Universitario de Materiales, Universidad de Alicante, Apartado 99, Alicante 03080, Spain*
[c]*Laboratory of Catalysis and Corrosion of Materials, Faculty of Sciences, University Chouaïb Doukkali, El Jadida, Morocco*

Received 1 May 2015; Accepted 11 October 2015

ABSTRACT

Cresols are phenolic pollutants found in industrial wastewaters. Their efficient removal is an important environmental concern. The isotherms and kinetics of the adsorption of an aqueous solution of o-Cresol, on a local Algerian Montmorillonite clay mineral (sodium clay (SC)) were determined experimentally. Various parameters influencing the adsorption were optimized, mainly the effect of the contact time, initial concentration and pH of the solution were studied. The experimental results obtained show that the equilibrium of sorption is reached within 15 min with a percentage of 99.507%. Indeed, the adsorbent dose is 15 mg with o-Cresol concentration of 62 mg/L, $T = 25^\circ\text{C}$ and pH 6.31 for the better adsorption. Results deducted from the adsorption isotherms also showed that the retention is predictable from these isotherms in agreement with the Langmuir model. Pseudo-second-order model describes the o-Cresol adsorption behavior with an intraparticle diffusion. In addition, the adsorption heat is around −31 kJ/K mol, which are in the limit between physical and chemical adsorption. The use of adsorptive properties of SC for the treatment of industrial wastewater seems to be an interesting solution.

Keywords: O-Cresol; Sodium clay; Adsorption; Kinetics; Environment

1. Introduction

Pollution of the environment in general and water pollution in particular, has attracted the attention of scientists about the subject of growing concern at the world level for the release of heavy metals, dyes, pesticides, phenols and other organic and inorganic compounds in the environment.

These chemical pollutants have serious consequences on the fauna, flora, and water courses [1,2]. Their presence in the water, even trace amounts, changes its flavor, color, and odor making it nonsuitable for consumption or toxic. Among the organic compound feared phenol and its derivatives.

Indeed, the first responsible for this pollution is industrialization, because technology development, several chemicals are produced and can be found in water, accidentally or by discharges.

---

*Corresponding author.

As the toxicity of these phenolic compounds is important, their concentration (up to several grams per liter) inhibits or reduces unfortunately microorganisms in plants treating wastewater [3]. The presence of phenols greatly reduced biodegradation of organic components [2,4], which makes the degradation of phenols very difficult.

The importance of protecting natural environments and improving water quality are increasing thanks to the inspection and monitoring of the environment in sounding the alarm on each health disaster proposing regulations increasingly stricts.

Cresols are phenols used as antiseptics and disinfectants. They also enter into the composition of many organic products: pesticides, antioxidants, phenolic resins [5,6]. Cresol is a mixture of three isomers of methylphenol (CH_3-C_6H_4OH) ortho-, meta-, and para-, which are unpleasant odor, but less toxic than ordinary phenol. These may produce very serious diseases like cancer or other pathologies [7–10].

Various techniques and methods of wastewater treatment are used to rid these contaminants. The most used physicochemical processes are as follows: coagulation, chemical precipitation, ion exchange, and adsorption [11–14] and membrane processes [15–17] and oxidation [18,19]. Their degradation by biological way [7,20–22], with the ability of many microorganisms to decompose, is a strategy widely used in organized detoxification of polluted environments.

Water treatment by adsorption is used for its efficiency in removing organic micro-pollutants [16,23]. Several studies have shown that adsorption on activated carbon is readily achievable [1,11,24]. However, the use of inexpensive adsorbents for water treatment is a subject of great interest [15,25]. Then, the elimination of phenolic pollutants from wastewater by inexpensive materials, such as natural or synthetic zeolites [12,13,26,27], the resins [28,29], and especially clays [16,30,31]. Today, clays are known by their abundance in nature [32,33], their ion-exchange properties and their high adsorption capacity [32–34]. Multiple physicochemical properties of clays give their properties quite remarkable: swelling, flexibility, plasticity, etc. They seem to be a better adsorbent to degrease and bleach wastewater polluted by industrial discharges [35], [42].

The objective of this work is to study this material in the removal of phenolic compounds as o-Cresol. The adsorption capacity is estimated by obtaining the adsorption isotherms and the kinetic of the process is also studied. The parameters of the adsorption process will be determined and optimized: the contact time, the initial concentration of the pollutant, or the pH of the aqueous solution.

2. Materials and methods

2.1. Adsorbent and adsorbate

Montmorillonite collected from Roussel, Hammam Boughrara (Maghnia located to the west of Algeria) has been used. This montmorillonite is commercial and it is provided by ENOF (National Company of the Non-ferrous Mining Products). The recovered solid phase was saturated with sodium ions by stirring in sodium bicarbonates ($NaHCO_3$). This clay has been called as sodium clay (SC).

The analysis of o-Cresol has been performed using the maximum wavelength of the UV–visible spectrum at $\lambda_{max} = 270$ nm.

2.2. Characterization methods

The montmorillonites have been characterized using different spectroscopic techniques (XRD, Fourier transform infrared spectroscopy (FTIR), BET) before and after adsorption. The X-ray diffractograms were made using a Bruker model diffractogram D8-Advance to the operating wavelength of the copper Kα ($\lambda = 1.5418$). FTIR was performed using a Bruker Alpha, over a range of 400–4,000 cm^{-1} with a resolution of 2 cm^{-1}. The specific surface of the adsorbents was determined by physical adsorption of nitrogen at 77 K using an Autosorb-6 equipment model (Quantachrome). The specific surface (S_{BET}) of adsorbent before and after adsorption was calculated using the BET equation (Brunauer–Emmett–Teller) assuming that the surface of the nitrogen molecule is 16.2 $Å^2$. The specific surface area, microporous volumes and pore size deduced from the data of adsorption–desorption isotherms of N_2 are, respectively, calculated according to the methods of Dubinin–Radushkevich (DR) and Barrett, Joyner and Halenda (BJH). The pH_{PZC} is defined as the pH for which there is neutral charge on the surface of the adsorbent. A volume (50 mL of sodium chloride solution (0.01 mol/L) was placed in capped bottles and the pH was adjusted from 2 to 12 by adding concentrated sodium hydroxide or hydrochloric acid. A 0.15 g of clay was then added to the NaCl solutions. After stirring magnetically for 48 h, the final pH was measured and plotted against the initial pH. The pH corresponding to the point of intersection with the pH (final) = pH (initial) was taken as the pH_{PZC} of the material [36,37].

2.3. Experimental protocol

The adsorption equilibrium was achieved by varying; the initial concentration of o-Cresol from 3.9 to

62.5 mg/L; the contact time was between 0 and 240 min; adsorbent mass from 10 to 50 mg; the pH was varied from 2 to 11; and the temperature between 6 and 70°C. The adsorbed amount of o-Cresol (q_e) (mg/g) was calculated using the following equation:

$$q_e = \frac{X}{m} = \frac{(C_i - C_{eq})V}{m} \tag{1}$$

Furthermore, the adsorption percentage is calculated using the following equation:

$$\%\,\text{adsorption} = \frac{(C_i - C_{eq})100}{C_i} \tag{2}$$

3. Results and discussion

3.1. Characterization of the adsorbent

Fig. 1 shows X-ray diffractograms of the raw clay (RC), SC, and the sodium clay after adsorption of o-Cresol (SCA), respectively. The predominant peaks in the raw bentonite are those of silica SiO_2 α-quartz ($2\theta = 21°$ and 27°), and those of the montmorillonite (6°, 17.5°, and 20°). Also, characteristic peaks of illite (9°, 20.70°, and 29.36°) are observed. Similar diffractograms were found by Konan [38]. Comparing these results with those of SC, it can be noted that the impurities, such as quartz, are largely eliminated during the Sodium homoionization. The sodium homoionization of the SC, induces the lowering of the reticular distance, from 19.24 to 16.69 Å. This decrease is due to the exchange of cations Ca^{2+}, Mg^{2+}, and K^+ by Na^+ ions which is smaller [36]. This confirms the good purification of the clay. On the other hand, in the diffractogram SCA, it can be observed an increase in d_{001} to 14.58 Å due to the presence of o-Cresol molecules incorporated into the interlayer space during the adsorption.

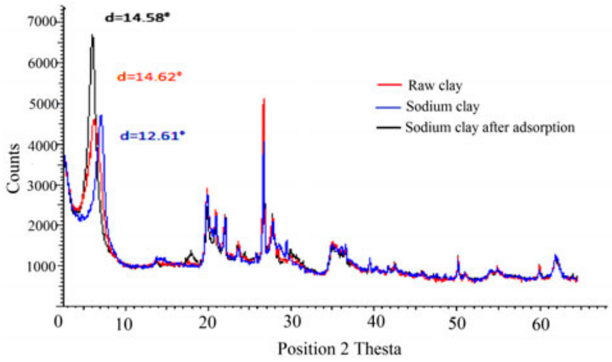

Fig. 1. XRD adsorbents RC, SC, and SCA.

The infrared spectra of the RC, SC and sodium clay after the adsorption of o-Cresol are shown in Fig. 2; the spectra show the presence of a band at 3,620 cm^{-1} attributed to the OH-Al, the band at 3,580 cm^{-1} to the Fe bond for OH of clays 2:1. Moreover, the band to 915 cm^{-1}, marks the deformation vibrations (bending) of the OH-Al bonds clay dioctahedral 2:1 [36].

The band centered around 1,630 cm^{-1} is assigned to the deformation vibrations of H_2O molecules adsorbed between the layers. Other bands at 875 and 1,460 cm^{-1} can be assigned to the vibration of carbonate ions CO_3^{2-}. Another band in the range 3,200–3,800 cm^{-1}, with an intense peak and shoulders at 3,400 and 3,625 cm^{-1} corresponds to the montmorillonite.

The comparison of the spectra of the RC and SC reveals a shift of the wave number of the band of OH groups centered around 1,634–1,632 cm^{-1} [39]. In addition, the appearance of the band situated at 1,460 cm^{-1} for the SC characteristic to the carbonates [39]. A displacement of the fine bands of stretching vibration of OH groups located at 3,620 cm^{-1} centered at 3,493 cm^{-1} and to 3,621 and 3,403 cm^{-1}, respectively [39].

The FTIR spectra of the SC before and after adsorption of o-Cresol (SC and SCA), respectively, show a decrease in the wave number of the band of OH groups located at 3,619 and 3,693 cm^{-1} and a weakening of the strong band between 900 and 1,200 cm^{-1} centered around 1,040 cm^{-1} corresponds to the stretching vibrations of Si–O bond. The spectra also detect a decrease and a shift of stretching vibration bands of OH groups centered around 1,632–1,634 cm^{-1}.

The BET surface area of RC is 34, 67 m^2/g for SC. Furthermore, the results show that the pore size distribution value of the SC 4.06 nm is higher than that the RC is 2.87 nm. An increase in the pore volume of 0.01 cm^3/g for RC to 0.04 cm^3/g for SC.

The pH_{pzc} values of RC and SC are 4.28 and 5.11, respectively. When the pH is less than the value of pH_{pzc}, the surfaces are charged positively when the pH is higher than the value of pH_{pzc}, the surfaces are negatively charged. Montmorillonite is positively charged at $pH < 5.11$ and negatively charged at $pH > 5.11$.

3.2. Adsorption kinetics

Fig. 3 shows the amount of o-Cresol adsorbed with time in an adsorption process for a concentration of o-Cresol of 62.5 mg/L. It can be observed that the

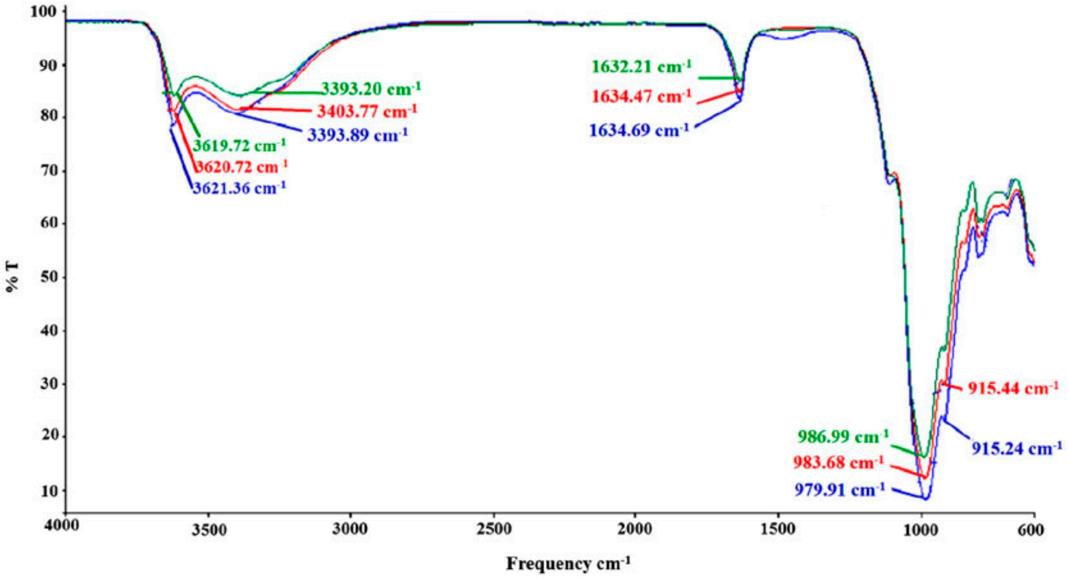

Fig. 2. FTIR spectra of samples RC, SC, and SCA.

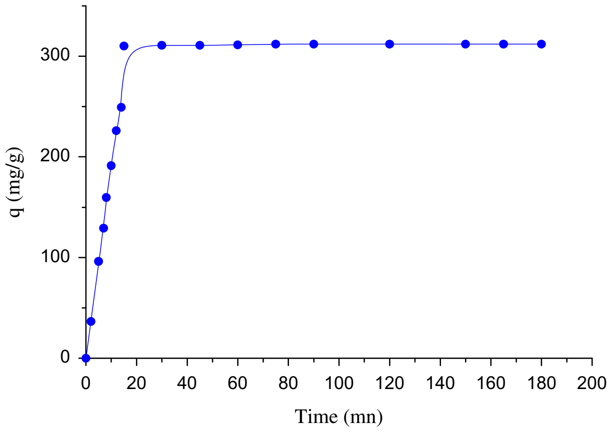

Fig. 3. Kinetics of adsorption of o-Cresol on SC ([*C*] = 62.5 mg/l; m (SC) = 50 mg; *T* = 25℃; pH 6.31).

equilibrium is reached very fast within 15 min. The maximum adsorption is achieved with an adsorption capacity of about over 300 mg/g. The other results were reported for the adsorption of o-Cresol, Adsorption of o-Cresol from dilute aqueous solution on bentonite clay treated by acid. The maximum adsorption capacitiy of o-Cresol was around 16.5 mg/g and the equilibrium was attained after 48 h [31]. Indeed, The removal of o-Cresol from water by the hybrid process of clay adsorption (Montmorillonite and kaolinite). Batch adsorption equilibrium experiments showed that the amount of adsorption for o-Cresol decreased in the order kaolin > montmorillonite. The maximum adsorption capacitiy of o-Cresol for kaolin and montmorillonite was an obout 8.4 and 7.98 mg/g, respectively, with a rapid initial step and reach equilibrium within 250 min. However, the adsorption of o-Cresol onto montmorillonite is faster than that onto kaolin [16].

3.3. *Effect of adsorbent dose*

To observe the effect of the dose of adsorbent (Fig. 4), the tests were carried out at different doses (15, 20, 30, 40, 50, and 100 mg/250 mL). From the results obtained in Fig. 5, the percentage of adsorption increases with increasing adsorbent dose. With 15 mg/250 mL of the clay, the adsorbed rate of the o-Cresol is very high as it reaches 99.5866%.

3.4. *Effet the pH of the medium*

Fig. 5 shows the effect of the pH in the adsorption capacity for a concentration of 62.5 mg/L for the SC. In the range of pH tested, the elimination of the o-Cresol using SC increases with pH up to pH 6.31 and then decreased significantly for more basic pH. The maximum adsorption is reached at pH 6.31.

It is well known that the properties of inorganic adsorbents are characterized by charges on its surface. The first type of reaction sites for clays is the silanol and aluminol groups Si–OH and Al–OH, respectively, and the charge of these groups depend on the pH of the solution [40]. The maximum amount adsorbed was found at pH 6.31. These results can be explained

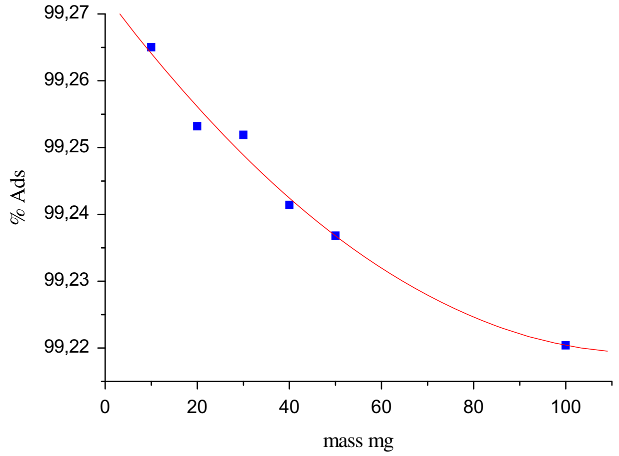

Fig. 4. Curve optimization of the adsorbent dose, Adsorption%—adsorbent dose ([C] = 62.5 mg/l; *t* = 15 mn; *T* = 25˚C; pH 6.31).

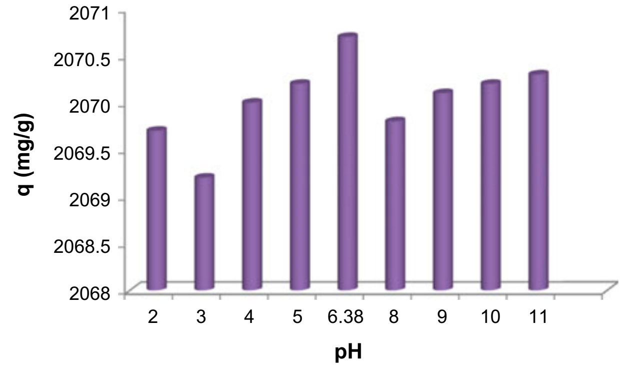

Fig. 5. Effect of solution pH on the adsorption of o-Cresol ([C] = 62.5 mg/l; *t* = 150 mn; m (SC) = 50 mg; *T* = 25˚C).

on the basis of the pH_{pzc} value of SC (5.11) and pKa of o-Cresol (10.26). At this pH range, o-Cresol exists in the molecular form and is basic in nature due to the electron releasing groups of methyl and hydroxyl [11]. Also, SC which has a net positive charge ($pH_{pzc} = 5.11$) has more affinity for the molecular form of o-Cresol and this results in its high adsorption uptake. Different results of pH were reported for the adsorption of o-Cresol on clays. A o-Cresol adsorption test showed that the maximum adsorption capacity of o-Cresol for Kaolin and Montmorillonite was an obout 8.4 and 7.98 mg/g at pH 9.1, respectively [16].

In too acidic conditions, the number of positively charged adsorption sites increases because the H^+ ions are then very mobile and occupy the active sites of the clay surface. In the basic conditions, the adsorption capacity decreases as a dominant negative charge on the clay surface cause repulsion with the o-Cresol.

3.5. Influence of temperature

To study the influence of temperature on the adsorption capacity of the o-Cresol on the adsorbent, a series of experiments was conducted at various temperatures: from 280 to 343 K is shown in Fig. 6. The amount of o-Cresol adsorbed reached a maximum after 15 min at a temperature of 25˚C. The variation of the temperature of the reaction medium affects slightly the adsorption of o-Cresol. When the temperature increases to 25˚C, the adsorption decreases which is probably for desorption.

3.6. Adsorption isotherm

Fig. 6 shows the adsorption isotherms of o-Cresol on SC were assessed by plotting the relation of q_e as a function of C_{eq} as illustrated (Fig. 7) after adsorption tests. The Langmuir model assumes monolayer adsorption, while the Freundlich model is empirical in nature which assumes the adsorption is heterogeneous on the surface [15,37].

The experimental data were analyzed according to the Langmuir and the Freundlich models (Figs. 8 and 9).

The Langmuir and Freundlich adsorption isotherm can be described by the following relations, respectively [35,37]:

$$\frac{C_{eq}}{q_e} = \frac{1}{K_L q_m} + \frac{C_{eq}}{q_m} \tag{3}$$

$$\log\ q_e = \log\ K_F + \frac{1}{n} C_{eq} \tag{4}$$

Fig. 7 clearly shows different adsorption capacities for the isotherm models in the nonlinear form of experimental data with both isotherm model (Langmuir and Freundlich). The linearized forms of the Langmuir

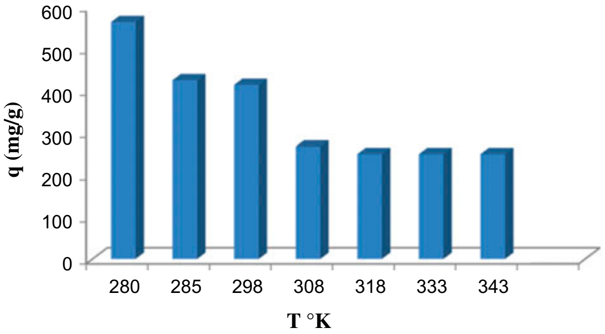

Fig. 6. Effect of temperature on the adsorption of o-Cresol ([C] = 62.5 mg/l; *t* = 150 mn; m (sc) = 50 mg; pH 6.31).

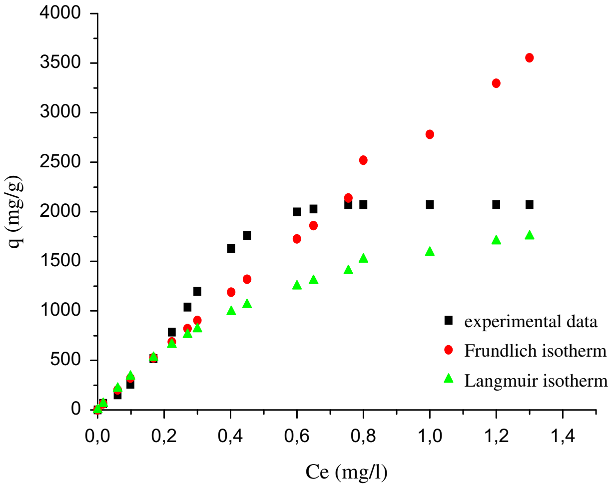

Fig. 7. Adsorption Isotherm of o-Cresol on SC.

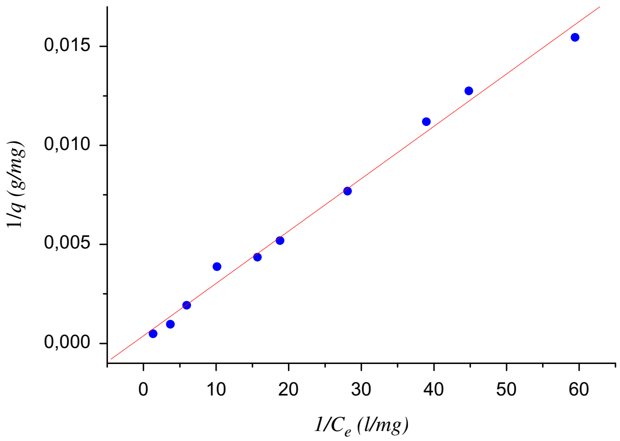

Fig. 8. Langmuir adsorption isotherm of o-Cresol on SC.

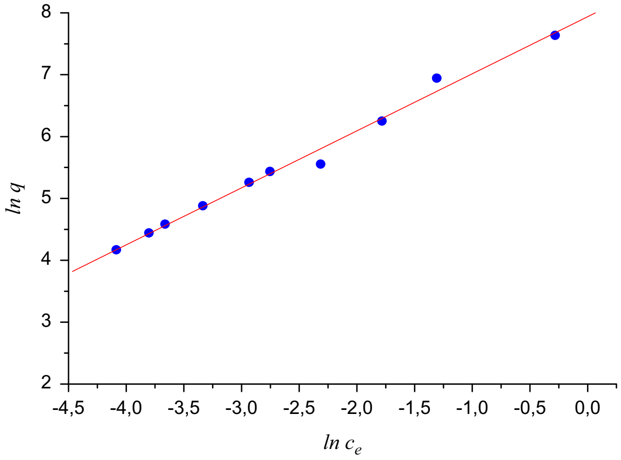

Fig. 9. Freundlich adsorption isotherm of o-Cresol on SC.

and the Freundlich models give correlation coefficients in the range of 0.98–0.99 (Table 1). A good linear regression was obtained for the Langmuir model confirm the results of the isotherm models in the nonlinear form. This indicates the probable formation of a

Table 1
The parameters of Langmuir and Freundlich isotherms

Adsorbat	O-Cresol
Adsorbate	Na-Clay
Langmuir isotherm	Freundlich isotherm
R^2 = 0.9936	R^2 = 0.9883
K_L = 1,46,272	K_F = 2,780, 51,099
q_m = 2,673, 6,538	n = 0.93424

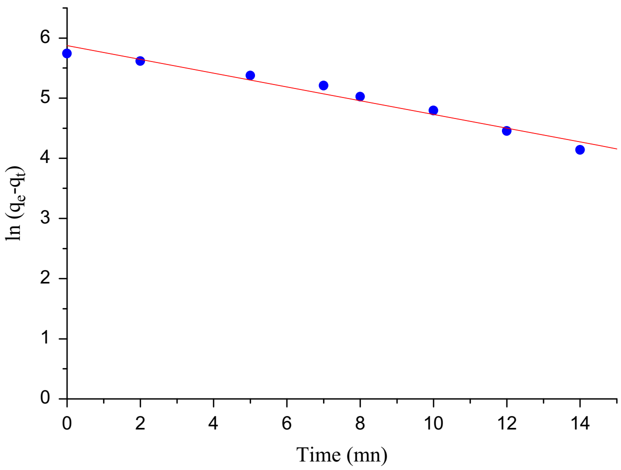

Fig. 10. Pseudo-first-order for the adsorption of the o-Cresol on SC.

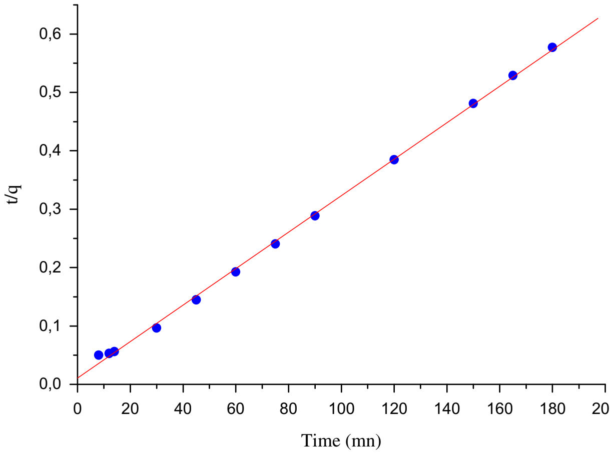

Fig. 11. Pseudo-second-order for the adsorption of the o-Cresol on SC.

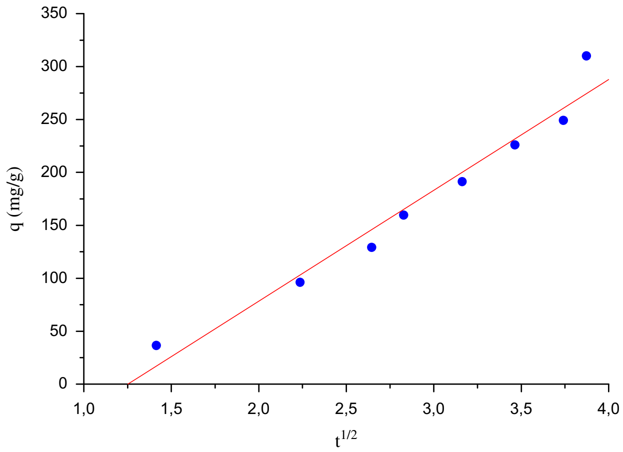

Fig. 12. Intraparticle diffusion for the adsorption of the o-Cresol on SC.

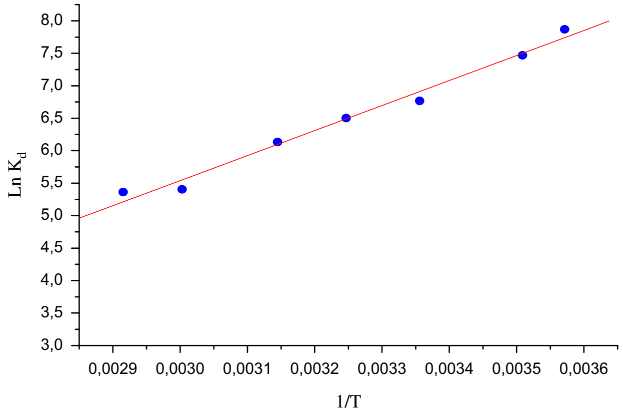

Fig. 13. ln K_d vs. $1/T$ for the adsorption of the o-Cresol on SC.

monolayer of dye without mutual interactions of localized sites whose energy is identical. The results compare competitively with some published results [14,16,17,31]. This may provide an advantage for developing countries local economies to use such low-cost adsorbents.

3.7. Kinetic analysis of o-Cresol

To better understand the adsorption mechanism of o-Cresol on SC, kinetic models of pseudo-first-order, pseudo-second-order [37,41], and the model of intraparticle diffusion [35,37] have was used in this study (Figs. 10, 11, and 12).

The equations of the first and second pseudo order were used to describe the adsorption reactions, using equations Lagergren:

$$\log(q_e - q_t) = \log(q_e) - \left(\frac{K_1}{2.303}\right)t \tag{5}$$

$$\frac{t}{q_t} = \left(\frac{1}{K_2 q_e^2}\right) + \left(\frac{1}{q_e}\right)t \tag{6}$$

Morris and Weber consider the evolution of the solute concentration in the solid phase follows a $t^{1/2}$ [43]:

$$q_t = \frac{X}{m} = K_{\text{diff}} t^{1/2} \tag{7}$$

3.8. Thermodynamic adsorption

The variation of the adsorption constant ln (K_d) as a function of $1/T$ allows to deduce the thermodynamic adsorption function like enthalpy and entropy (ΔH and ΔS) (Fig. 13).

Table 2 shows the obtained values for these parameters. The analysis of the results in indicates that the adsorption of the o-Cresol is spontaneous. Negative values of ΔH which are less than 40 kJ/mol suggest that the process of physical adsorption appears to be exothermic as corresponds to an adsorption process. In addition, the entropy values are negative low near zero, resulting in increased mobility of adsorbed species. These findings are in agreement with those obtained by the results of m-Cresol adsorption on activated carbon [14].

Table 2
Thermodynamic parameters of adsorption

Adsorbat o-Cresol
Adsorbate Na-Clay

T°K	280	285	298	308	318	333	343
ln K_d	7,86,853,896	7,46,855	6,76,609	6,50,263	6,13,369	5,40,332	5,362,367
ΔG (kJ/K mol)	−18,01,395	−17,7,636	−17,1,129	−16,6,124	−16,1,118	−15,3,611	−14,8,605
ΔS (kJ/mol)	−0.05005						
ΔH (kJ/K mol)	−32.02922						

4. Conclusion

The elimination of organic pollution by the conventional treatment is not sufficient, in particular for the water contaminated by organic compound. Processes using adsorption then often constituted of a technical choice. The aim of our study was to investigate the specific adsorption performance of montmorillonite toward organic compounds o-Cresol present in industrial effluents.

The effect of some experimental parameters was studied using a batch adsorption technique. The results showed that the time required for complete adsorption and equilibrium is reached very fast within 15 min. With 15 mg of the clay, the adsorbed o-Cresol rate is very high as it reaches 99.58%. The best rate is obtained when the pH is neutral 6.31. The kinetic analysis indicates fast reactions with a second-order kinetics and intra-particle diffusion. The adsorption of o-Cresol is exothermic and spontaneous, and of a physical type. The results deduced from the plot of the adsorption isotherms of o-Cresol shows that retention is predictable from these isotherms in agreement with the Langmuir model.

Finally, the SC proves to be a best adsorbent to remove the micro-pollutant o-Cresol from industrial wastewater.

Acknowledgments

Financial support for this work by the Directorate General of Scientific Research and Technological Development (DGRSDT) of Algeria is gratefully appreciated. The authors thank the staff of Servicios Técnicos de Investigación (SSTTI) of the University of Alicante for characterization assistance.

Nomenclature

RC — raw clay
SC — sodium clay
C_i — initial concentration of the pollutant (mg/L)
C_eq — concentration at equilibrium adsorbate (mg/L)
k_d — distribution constant of adsorption
k_1 — constant rate of pseudo-first-order adsorption (g/mg min)
k_2 — constant rate of pseudo-first-order adsorption (g/mg min)
K_L and K_F — adsorption constants of Langmuir and Freundlich
K_diff — intraparticle diffusion coefficient (mg/(g min))
q_e — amount of o-Cresol adsorbed at equilibrium (mg/g)
q_m — maximum adsorption capacity (mg/g)
q_t — amounts of o-Cresol adsorbed at the time t (mg/g)
m — mass of the adsorbent (g)
SCA — sodium clay after adsorption
V — volume of the solution (L)
X — number of grams of o-Cresol adsorbed (mg)
λ_max — maximum wavelength of absorption of o-Cresol
ΔH_ads — enthalpy
ΔS_ads — entropy
ΔG — free energy of adsorption

References

[1] R.F. Christman, R.A. Minear, Organics in Lakes, in: J.P. Fant (Ed.), Organic Compounds in Aquatic Environments, Marcel Debber, New York, NY, 1971, pp. 119–143.

[2] N. Shivaraman, R. Pandey, Characterization and biodegradation of phenolic wastewater, J. Indian Assoc. Environ. Manage. 27 (2000) 12–15.

[3] Z. Duan, Microbial degradation of phenol by activated sludge in a batch reactor, Environ. Prot. Eng. 37 (2011) 53–63.

[4] B. Marrot, A. Barrios-Martinez, P. Moulin, N. Roche, Biodegradation of high phenol concentration in a membrane bioreactor, Int. J. Chem. React. Eng. 6 (2008) 1–12.

[5] H.L. Jiang, J.H. Tay, A.M. Maszenan, S.T.L. Tay, Bacterial diversity and function of aerobic granules engineered in a sequencing batch reactor for phenol degradation, Appl. Environ. Microbiol. 70 (2004) 6767–6775.

[6] S. Yi, W.Q. Zhuang, B. Wu, S.T.L. Tay, J.H. Tay, Biodegradation of p-nitrophenol by aerobic granules in a sequencing batch reactor, Environ. Sci. Technol. 40(7) (2006) 2396–2401.

[7] A.W. Martinez, N.S. Recht, T.H. Hostetter, T.W. Meyer, Removal of P-Cresol sulfate by hemodialysis, J. Am. Soc. Nephrol. 16 (2005) 3430–3436.

[8] H. Boszczyk-Maleszak, M. Chorazy, E. Bieszkiewicz, J. Kacieszczenko, Phenol utilisation by fungi isolated from activated sludge, Acta Microbiol. Pol. 51(183) (2002) 183–187.

[9] V. Kavitha, K. Palanivelu, The role of ferrous ion in Fenton and photo-Fenton processes for the degradation of phenol, Chemosphere 55 (2004) 1235–1243.

[10] Y.S. Peng, Y.T. Lin, S.D. Wang, K.Y. Hung, Y. Chen, S.M. Wang, p-Cresol induces disruption of cardiomyocyte adherens junctions, Toxicology 306 (2013) 176–184.

[11] V.K. Gupta, A. Nayak, S. Agarwal, I. Tyagi, Potential of activated carbon from waste rubber tire for the adsorption of phenolics: Effect of pre-treatment conditions, J. Colloid Interface Sci. 417 (2014) 420–430.

[12] J. Vijayakumar, S.K. Chikkala, S. Mandal, S. Mayadevi, Adsorption of cresols on zinc-aluminium hydroxides—A comparison with zeolite-X, Sep. Sci. Technol. 46(3) (2011) 483–488.

[13] L. Narasimhan, B. Kuchta, O. Schaef, P. Brunet, P. Boulet, Mechanism of adsorption of p-cresol uremic toxin into faujasite zeolites in presence of water and sodium cations—A Monte carlo study, Microporous Mesoporous Mater. 173 (2013) 70–77.

[14] L.J. Kennedy, J.J. Vijaya, G. Sekaran, K. Kayalvizhi, Equilibrium, kinetic and thermodynamic studies on the adsorption of m-cresol onto micro- and mesoporous carbon, J. Hazard. Mater. 149(1) (2007) 134–143.

[15] M. Anbia, A. Ghaffari, Adsorption of phenolic compounds from aqueous solutions using carbon nanoporous adsorbent coated with polymer, Appl. Surface Sci. 255 (2009) 9487–9492.

[16] S.H. Lin, R.C. Hsiao, R.S. Juang, Removal of soluble organics from water by a hybrid process of clay adsorption and membrane filtration, J. Hazard. Mater. 135 (2006) 134–140.

[17] V. Wernert, O. Sch¨af, V. Faure, P. Brunet, L. Doub, Y. Berland, P. Boulet, B. Kuchta, R. Denoye, Adsorption of the uremic toxin p-cresol onto hemodialysis membranes and microporous adsorbent zeolite silicalite, J. Biotechnol. 123 (2006) 164–173.

[18] M.Pimentel, Studies of the oxidation of phenol and cresols by advanced electrochemical oxidation in a homogeneous medium Application to the aviation industry effluent treatment, Phd thesis, University of Paris-Est Marne-la-Vallée, 2008.

[19] J.A. Jiang, J.L. Du, D.H. Liao, Z.G. Wang, Y.F. Ji, Efficient $Co(OAc)_2$-catalyzed aerobic oxidation of EWG-substituted 4-cresols to access 4-hydroxybenzaldehydes, Tetrahedron Lett. 55 (2014) 1406–1411.

[20] M. Hernández-Esparza, M.C. Doria-Serrano, G. AceroSalinas, F.A. Ruiz-Treviño, Removal of high phenol concentrations with adapted activated sludge in suspended form and entrapped in calcium alginate/cross-linked poly(N-vinyl pyrrolidone) hydrogels, Biotechnol. Prog. 22 (2006) 1552–1559.

[21] S.S. Adav, M.Y. Chen, D.J. Lee, N.Q. Ren, Degradation of phenol by aerobic granules and isolated yeast *Candida tropicalis*, Biotechnol. Bioeng. 96(5) (2007) 844–852.

[22] Y. Ren, L. Peng, G. Zhao, C. Wei, Degradation of m-cresol via the ortho cleavage pathway by *Citrobacter farmeri* SC01, Biochem. Eng. J. 88 (2014) 108–114.

[23] E. Titus, A.K. Kalkar, V.G. Gaikar, Adsorption of anilines and cresols on NaX and different cation exchanged zeolites (equilibrium, kinetic, and IR investigations), Sep. Sci. Technol. 37(1) (2002) 105–125.

[24] R.H. Toh, P.E. Lim, C.E. Seng, R. Adnan, Immobilized acclimated biomass-powdered activated carbon for the bioregeneration of granular activated carbon loaded with phenol and o-cresol, Bioresour. Technol. 143 (2013) 265–274.

[25] R.K. Singh, S. Kumar, S. Kumar, A. Kumar, Development of parthenium based activated carbon and its utilization for adsorptive removal of *p*-cresol from aqueous solution, J. Hazard. Mater. 155 (2008) 523–535.

[26] A. Kuleyin, Removal of phenol and 4-chlorophenol by surfactant-modified natural zeolite, J. Hazard. Mater. 144 (2007) 307–315.

[27] Z. Aksu, J. Yener, A comparative adsorption/biosorption study of mono-chlorinated phenols onto various sorbents, Waste Manage. 21 (2001) 695–702.

[28] B.C. Pan, X. Zhang, W.M. Zhang, J.Z. Zheng, B.J. Pan, J.L. Chen, Q.X. Zhang, Adsorption of phenolic compounds from aqueous solution onto a macroporous polymer and its aminated derivative: Isotherm analysis, J. Hazard. Mater. 121 (2005) 233–241.

[29] K. Abburi, Adsorption of phenol and p-chlorophenol from their single and bisolute aqueous solutions on Amberlite XAD-16 resin, J. Hazard. Mater. 105 (2003) 143–156.

[30] F.A. Banat, B. Al-Bashir, S. Al-Asheh, O. Hayajneh, Adsorption of phenol by bentonite, Environ. Pollut. 107 (2000) 391–398.

[31] M.A. Hassan, H.M. Eissa, A.M. Mohammed, Adsorption of phenol and o-Cresol from dilute aqueous solution on bentonite clay, J. Int. Environ. Appl. Sci 6(4) (2011) 547–552.

[32] A. Ramdani, S. Taleb, A. Benghalem, N. Ghaffour, Removal of excess fluoride ions from Saharan brackish water by adsorption on natural materials, Desalination 250 (1) (2010) 408–413.

[33] A. Ramdani, S. Taleb, A. Benghalem, Study of the optimization of the potential of adsorption of the local montmorillonite for the reduction of the excess of ions Fluorides of Saharan water, Phys. Chem. News 52 (2010) 89–97.

[34] R. Sennour, G. Mimane, A. Benghalem, S. Taleb, Removal of the persistent pollutant chlorobenzene by adsorption onto activated montmorillonite, Appl. Clay Sci. 43 (2009) 503–506.

[35] I. Feddal, A. Ramdani, S. Taleb, E.M. Gaigneaux, N. Batis, N. Ghaffour, Adsorption capacity of methylene blue, an organic pollutant, by montmorillonite clay, Desalin. Water Treat. 52 (2014) 2654–2661.

[36] A. Zehhaf, Studies of adsorption and adsorption of electro-toxic metals in the surface water on various adsorbents, PhD thesis, Applied Physical Chemistry, University of Mascara, 2012.

[37] A. Ouldmoumna, L. Reinert, N. Benderdouche, B. Bestani, L. Duclaux, Characterization and application of three novel biosorbents "*Eucalyptus globulus*, *Cynara cardunculus*, and *Prunus cerasefera*" to dye removal, Desalin. Water Treat. 51 (2013) 3527–3538.

[38] K.L. Konan, Interactions between clay minerals and calcium-rich basic medium, PhD thesis, University of Limoges. Doctoral School Science—Technology—Health, Faculty of Science and Technology Study Group Heterogeneous Materials, 2006.

[39] A. Ramdani, Reduced salinity of Saharan brackish water by fluoride ions retention on activated natural materials: Comparison with membrane processes, PhD thesis, Applied Physical Chemistry, University of Djillali LIABES Sidi-Bel-Abbes, 2012.

[40] D.M. Manohar, B.F. Noeline, T.S. Anirudhan, Adsorption performance of Al-pillared bentonite clay for the removal of cobalt(II) from aqueous phase, Appl. Clay Sci. 31 (2006) 194–206.

[41] M. Mourabet, A. El Rhilassi, M. Bennani-Ziatni, R. El Hamri, A. Taitai, Studies on fluoride adsorption by apatitic tricalcium phosphate (ATCP) from aqueous solution, Desalin. Water Treat. 51 (2013) 6743–6754.

[42] A. Tor, Removal of fluoride from an aqueous solution by using montmorillonite, Desalination 201 (2006) 267–276.